

PARALLEL-MIDDLE-BODY AND STERN-FORM RELATIVE SIGNIFICANCE IN THE WAKE FORMATION OF SINGLE-SCREW LARGE SHIPS

Ketut Suastika^{1*}, Fajar Nugraha², I Ketut Aria Pria Utama¹

¹*Department of Naval Architecture and Shipbuilding Engineering, Faculty of Marine Technology, Institut Teknologi Sepuluh Nopember (ITS), Kampus ITS Sukolilo, Surabaya 60111, Indonesia*
²*PT. Biro Klasifikasi Indonesia (BKI), Jl. Yos Sudarso 38-40, Tanjung Priok, Jakarta 14320, Indonesia*

(Received: March 2016 / Revised: November 2016 / Accepted: January 2017)

ABSTRACT

The relative significance of the parallel middle body and stern form in the wake formation of single-screw large ships and their contribution to the ship's viscous resistance are studied by using computational fluid dynamics (CFD). A 10450-DWT tanker is considered by varying the ratio of the parallel-middle-body's length to the ship's length (L_{mb}/L) and by varying the shape of the stern form from a V-like to a U-like underwater stern transom section. In all the calculations, the principal dimension and the displacement of the ships are kept constant. A larger value for the parallel-middle-body relative length (L_{mb}/L) of ships with the same stern form results in a larger drag coefficient but does not affect the nominal wake fraction significantly. A change in the shape of the underwater stern form, from a V-like to a U-like section, results in a much larger drag coefficient ascribed to the much larger wake fraction. The stern form dominantly affects the nominal wake fraction and the ship's viscous resistance compared to the parallel-middle-body relative length.

Keywords: CFD; Parallel middle body; Ship resistance; Stern form; Wake fraction

1. INTRODUCTION

A ship moving in the water generates a wake behind it. This wake affects the ship's resistance and the efficiency of the ship's propeller, and should thus be considered carefully in the early stage of the ship-design process to obtain an economical ship with a good propulsive performance. Due to the wake, the water velocity heading to the propeller, the so-called advanced velocity, is generally smaller than the ship's speed. A parameter characterizing the wake field is the wake fraction, which is termed "nominal wake fraction" in the case without any working propeller.

Earlier studies have shown that the nominal wake fraction is a function of the frictional coefficient, which is in turn a function of the Reynolds number (Benedek & Balogh, 1968; Dyne, 1974; Eca & Hoekstra, 2009). More recently, Wang et al. (2015) found a linear relationship between the reciprocal value of the nominal wake fraction and the Reynolds number in logarithmic scale. A larger value for the wake fraction results in a less efficient propeller. Thus, a ship with a larger wake fraction will generally require more power (relatively uneconomical ship) than a similar ship (with the same displacement) with a smaller wake fraction to achieve the same speed (Choi et al., 2009, Choi et al., 2010; Seo et al., 2010).

*Corresponding author's email: k_suastika@na.its.ac.id, Tel. +62-31-5947254, Fax. +62-31-5964182
Permalink/DOI: <https://doi.org/10.14716/ijtech.v8i1.3542>

When considering the ship's hull form, Guldhammer (1962) provided the hull form data of typical ships, and later, ship-hull optimization methods were proposed by different authors. Zhao et al. (2015) proposed a ship-hull optimization method by minimizing the ship's resistance using a wavelet method. Kostas et al. (2015) proposed a ship-hull optimization method using a T-spline-based BEM-isogeometric solver. For the special gulet hull form, Aydin (2013) systematically developed a series for this hull type generated from 21 Turkish gulets with cruiser sterns. Huang & Yang (2016) developed an integrated hydrodynamic optimization tool for the simulation-based design of hull forms for reduced drag.

The stern form clearly affects the wake formation behind the ship and, thus, affects the ship's resistance. A ship with a V stern section generally has a smaller resistance than ships with U or bulbous sections do. On the other hand, the V section results in less uniform inflow to the propeller compared to the U or bulbous stern forms (Holden et al., 1980; Hoyle et al., 1986).

In addition to the stern form, the relative length of the parallel middle body of relatively large ships will also affect the wake formation behind the ship by affecting the thickness of the turbulent boundary layer. The purpose of the present study is to quantify the relative significance of the parallel-middle-body relative length and stern form in the wake formation behind the ship and their contribution to the ship's resistance. The nominal wake fraction, according to Taylor's definition, is used as a parameter to characterize the ship's wake.

2. METHODOLOGY

A 10450-DWT tanker is considered in a study using computational fluid dynamics (CFD). The success of the CFD method in predicting the wake field, the ship's resistance, and its propulsion performance has been demonstrated in many earlier studies (e.g. Larsson et al., 2003; Park et al., 2013; Wang et al., 2015). The ship particulars are summarized in Table 1. The hull form is derived from Guldhammer's form data (Guldhammer, 1962), which are deemed adequate for the present purpose. It is simpler than the methods proposed by, for example, Zhao et al. (2015) or Kostas et al. (2015). The body plan and profiles of the tanker are shown in Figure 1.

Table 1 Ship particulars (10450-DWT tanker)

Length between perpendiculars (L_{pp})	117.45 m
Water-line length (L_{wl})	122.14 m
Beam (B)	19.0 m
Height (H)	10.5 m
Draft (T)	7.8 m
Displacement (Δ)	13797 ton
Service speed (V_s)	14 knot

To study the relative significance of the parallel-middle-body relative length (L_{mb}/L) and the stern form on the nominal wake fraction and the ship's resistance, the relative length of the parallel middle body and the stern form are varied for the five cases that are considered, as summarized in Table 2. In the calculations, the water-line length L_{wl} is used to represent the ship's length L . Case 1 is the basic case, for which the body plan and profiles are shown in Figure 1. The stern forms I, II, and III are increasingly abrupt, from V-like to U-like underwater stern sections, as shown in Figures 2a–2c. In Cases 1, 2, and 3, the ships have the same stern form but different parallel-middle-body relative lengths. In Cases 3, 4, and 5, the ships have the same parallel-middle body relative length but different stern forms.

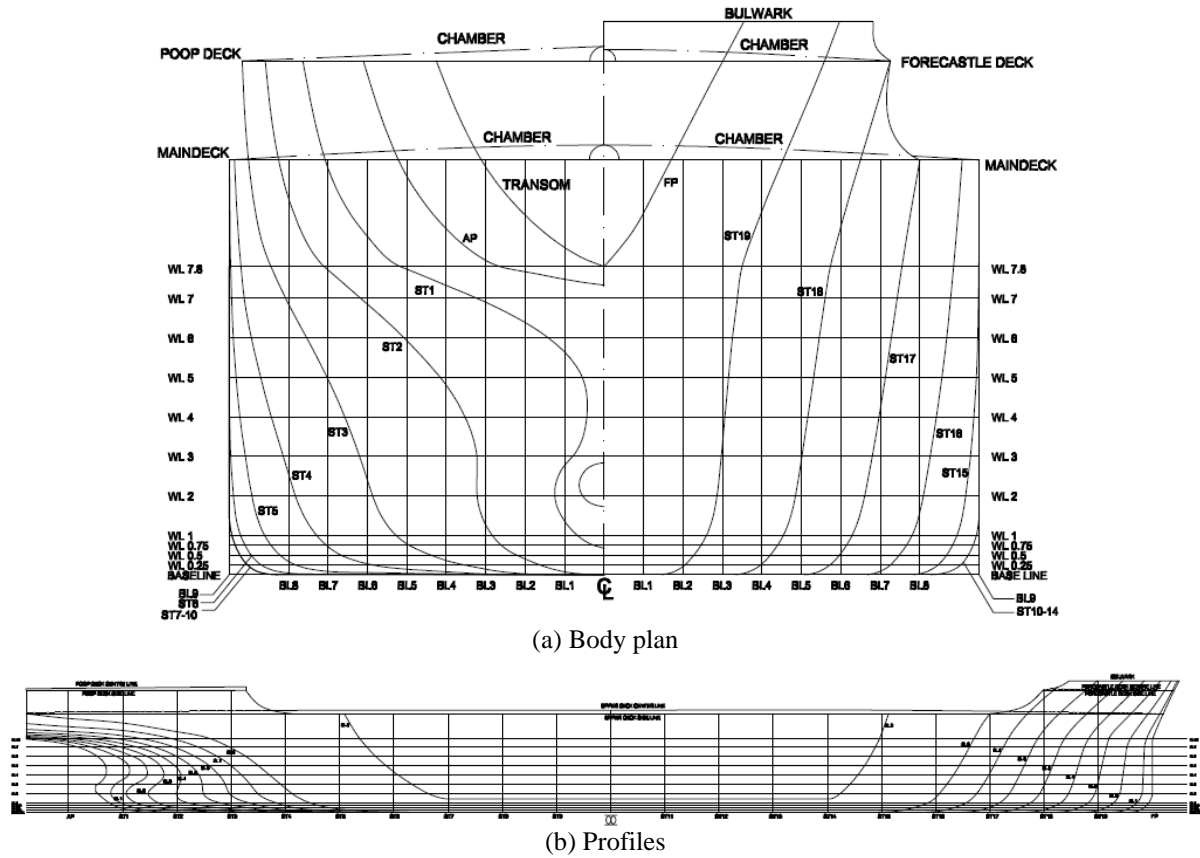


Figure 1 Body plan and profiles of the 10450-DWT tanker: (a) body plan; and (b) profiles

Table 2 Cases considered in the study

Case	L_{mb}/L	Stern form
1	0.11	I
2	0.34	I
3	0.46	I
4	0.46	II
5	0.46	III

The hull form from the midship toward the bow is the same in all five cases and so is the length of the forward parallel middle body. To obtain variations in the parallel-middle-body relative length, only the length of the aft parallel middle body is varied. The forward parallel middle body will mainly affect the pressure resistance while the aft parallel middle body will mainly affect the wake. By using the same length for the forward parallel middle body in all cases, the effect of the aft parallel middle body (wake) can be isolated.

Five models representing the five cases were generated and run serially in a computer with an intel® Core™ i5-3470 3.20 GHz processor with 4 GB RAM in a 64-bit Windows 7 Professional operating system. The average time required for running the model simulation was approximately two and a half hours. In all the models, the ship displacements are kept constant. This is achieved by adapting the hull form systematically and at the same time calculating the ship’s hydrostatics with the aid of the numerical tool Maxsurf.

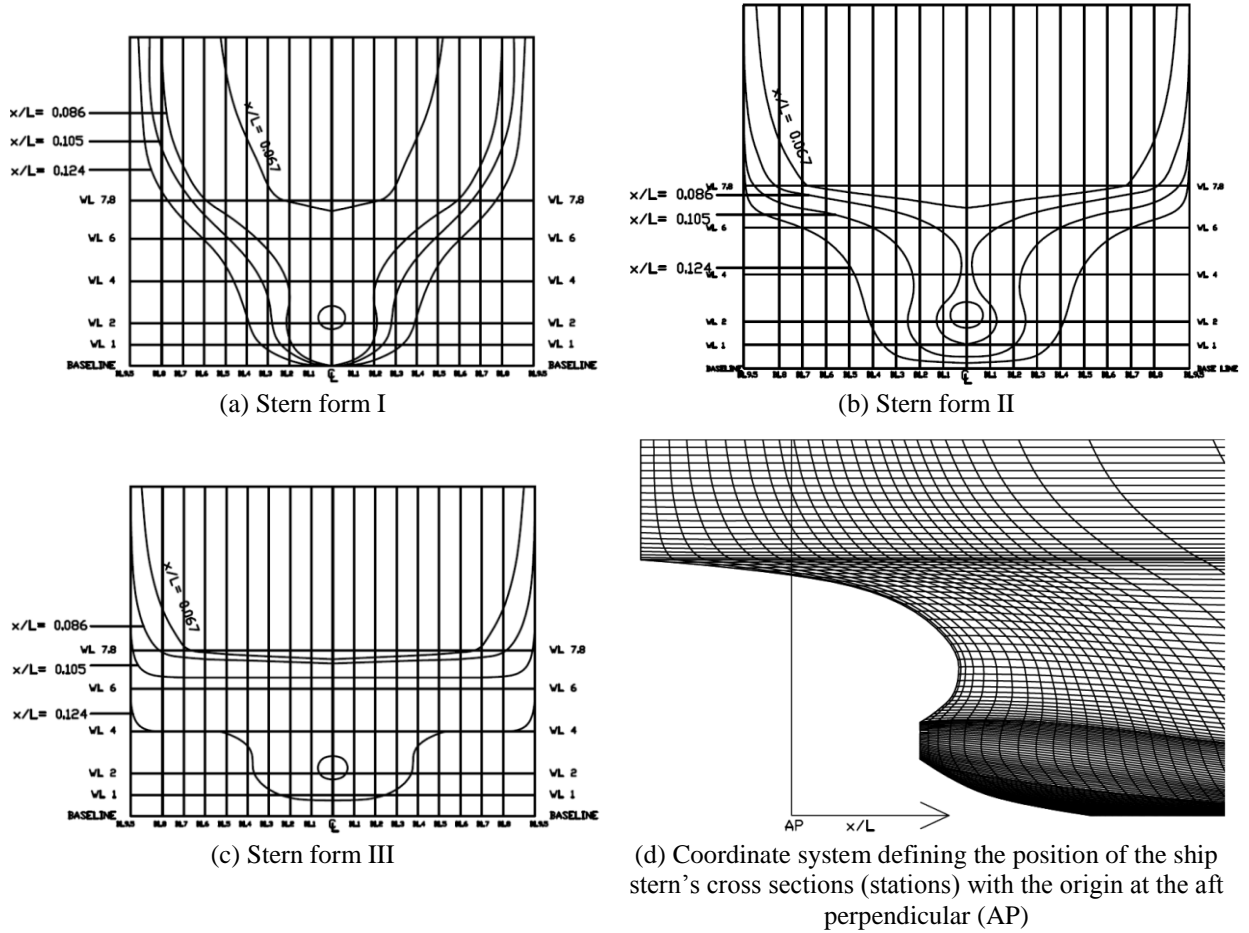


Figure 2 Body plans of: (a) stern form I; (b) stern form II; (c) stern form III; and (d) the used coordinate system

The nominal wake fraction w is obtained from the calculated axial flow velocity behind the ship using Taylor’s definition as follows:

$$w = \frac{V_s - V_a}{V_s} \tag{1}$$

where V_s is the ship’s speed and V_a is the advanced speed.

2.1. Meshing, Boundary Conditions, and the Turbulence Model

A right-handed coordinate system (x, y, z) is defined with the positive x -direction in the forward direction, the positive y -direction in the port direction, and the positive z -direction vertically upward. A non-uniform mesh with a structured grid is employed. The number of cells (elements) used in the simulations varies from 1.5×10^6 for Case 1 to 3.9×10^6 for Case 5, depending on the fulfilment of the grid-independence criterion (specified below). Parts of the hull mesh are shown in Figure 3, which shows stern forms I, II, and III.

The boundary conditions of the computational domain are defined as follows (Versteeg & Malalasekera, 2007). The inlet boundary, located $1.5-L$ upstream from the ship, is given as a uniform flow with the velocity equaling the ship’s speed. The outlet boundary, at a location $2-L$ downstream from the ship, is given as the pressure equaling the undisturbed static pressure, ensuring no upstream propagation of disturbances (Mitchel et al., 2008). The boundary condition on the hull surface is defined as the no-slip boundary and with the (parallel to the

flow direction) horizontal and vertical walls bounding the flow domain as a free-slip boundary. Free surface effects (the generation of waves) are not included in the present study. Earlier studies have shown that free surface effects are relatively small on the nominal wake field (Dymarski & Kraskowski, 2010; Wang et al., 2015). Therefore, to reduce the time of convergence, the wake contribution due to waves is ignored. Thus, the ship's wake is due to the pressure (potential) and viscous effects.

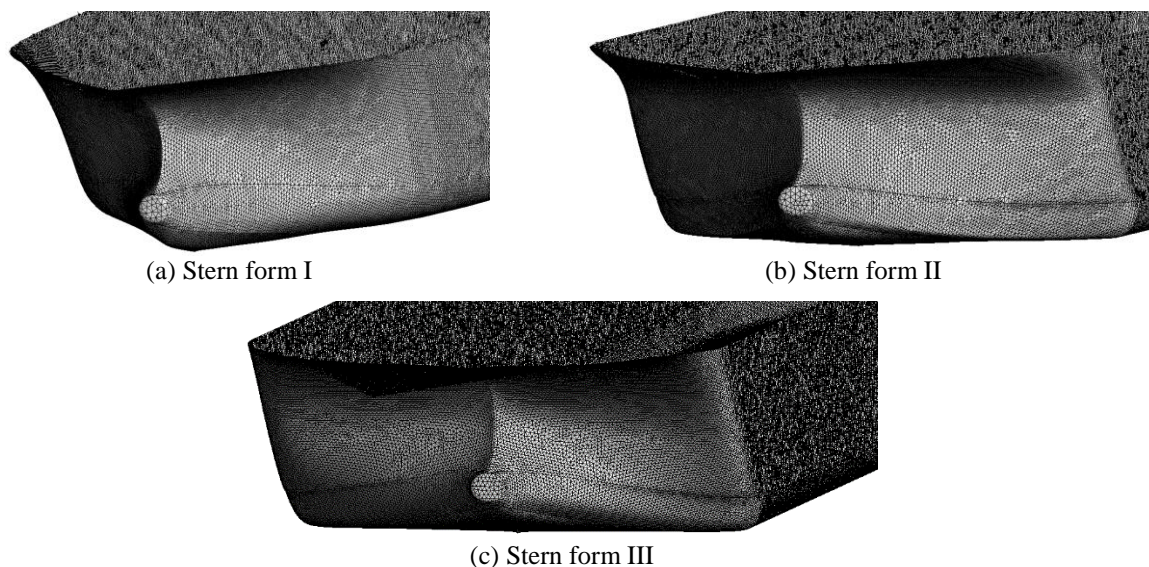


Figure 3 Parts of the hull meshes showing: (a) stern form I; (b) stern form II; and (c) stern form III

The choice of turbulence model is crucial in simulations of wake fields. The turbulence model used in the present study is the SST $k-\omega$ model (Menter, 1994). Such a model has been successfully applied in previous numerical studies on wake fields (Wang et al., 2015) and in the prediction of ship resistance components (Banks et al., 2010). The viscous-flow field is solved using Reynold's averaged Navier–Stokes (RANS) solver for incompressible flow.

2.2. Convergence and Grid-independence Criteria

Tests were performed so that the numerical results (flow velocities and the ship's resistance) complied with the convergence and grid-independence criteria. The root mean square (RMS) error criterion with a residual target value of 10^{-4} is used as the criterion for the convergence of the numerical solutions.

Table 3 A summary of the calculation results for ship resistance using a different number of elements for Case 2

Number of elements	Ship resistance (N)	Resistance difference percentage (%)
10395	859505	-
21610	629853	36.5
40027	496942	26.7
84854	379197	31.1
162200	326188	16.3
380399	279978	16.5
720736	261955	6.9
1571226	247624	5.8
3191720	244599	1.2

The grid-independence criterion is defined such that the difference between two subsequently calculated ship resistances, the latter calculation using a number of cells (elements) approximately twice that used in the former, is less than 2% (Anderson, 1995). To illustrate this, Table 3 shows a summary of ship resistance calculations using a different number of elements for Case 2. In this case, using 1,571,226 elements (approximately 1.6 million) in the simulation fulfils the grid-independence criterion, as stated above.

3. RESULTS AND DISCUSSION

Figure 4 shows the results of the wake fraction w as a function of the normalized position behind the ship x/L . Figure 4 shows that the wake fraction decreases monotonically in the downstream direction. In all cases, it approaches zero at locations $x/L > 0.26$. A study previously reported by Melville-Jones (1937) and later confirmed by Utama (1999) indicated that the wake effect behind the ship disappears at a position approximately $0.3L$ behind the vessel. This is in good agreement with the present findings.

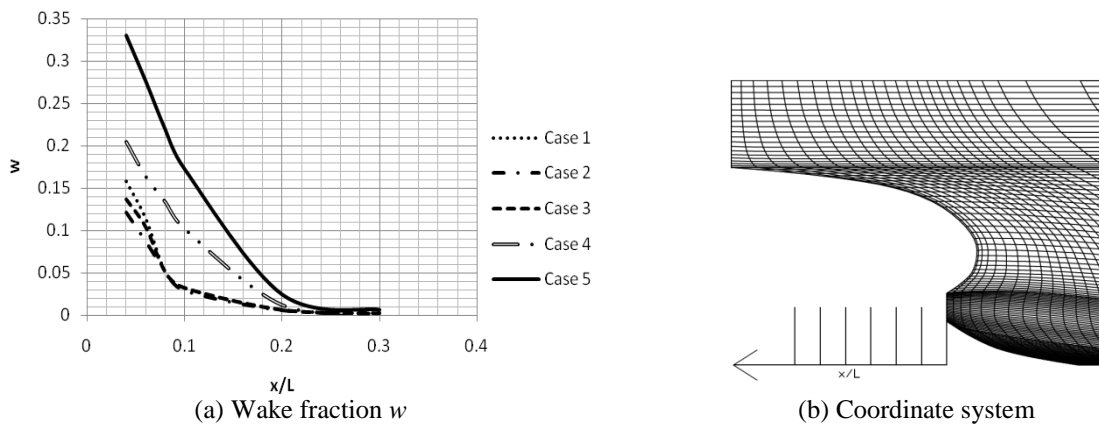


Figure 4 (a) Wake fraction w as a function of the normalized position x/L behind the ship for the five cases considered; and (b) the coordinate system

Furthermore, the wake fraction at a given location behind the ship increases significantly for ships with an increasingly abrupt stern form (from a V-like to a U-like form; Cases 3, 4, and 5), consistent with the results of previous studies (Hoekstra, 1975; Holden et al., 1980). On the other hand, the difference in wake fractions for ships with the same stern form but with an increasing parallel-middle-body length (Cases 1, 2, and 3) is relatively small. Their values are approximately the same at locations $x/L > 0.07$ (a difference is only observed for $x/L < 0.07$). As shown in Figure 4, Case 2 with a parallel-middle-body relative length $L_{mb}/L = 0.34$ results in the smallest wake fraction. Although there is an optimum value for the parallel-middle-body relative length that will result in the smallest wake fraction ($L_{mb}/L = 0.34$ for the cases studied), its influence on the wake fraction is relatively small compared to the influence of the ship's stern form. Clearly, the ship's stern form affects the wake fraction much more significantly than the parallel-middle-body relative length does.

The above findings are consistent with the calculated pressure distribution on the hull stern (see Figures 5a–5e). There is a significant increase in the pressure on the hull stern for increasingly abrupt stern forms (Cases 3, 4, and 5). Furthermore, the difference in pressure distribution for Cases 1, 2, and 3 is rather small and the pressure is smaller than that in Cases 4 and 5. From among Cases 1, 2, and 3, Case 2 has the smallest pressure.

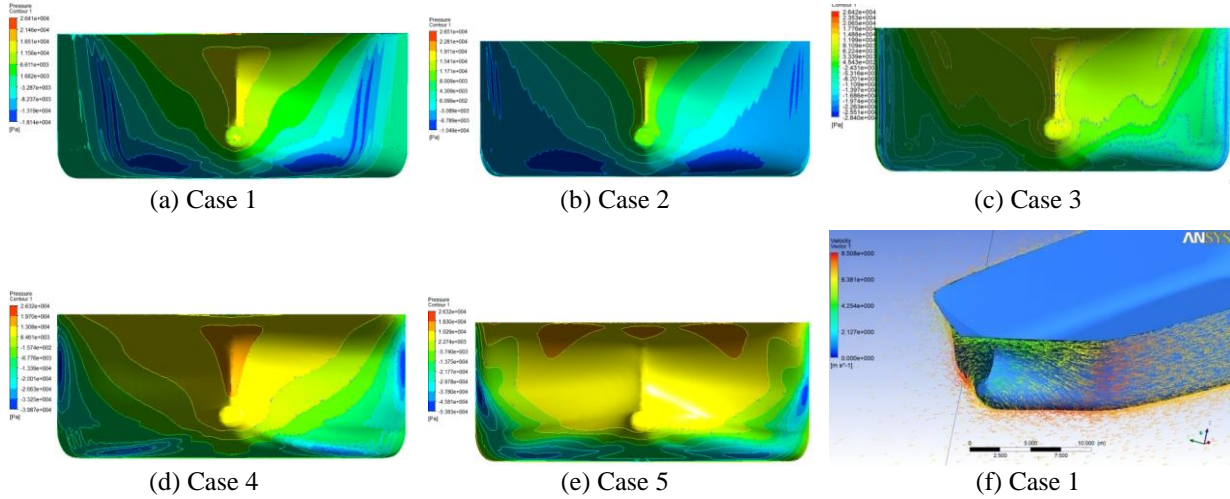


Figure 5 Dynamic pressure distribution on the hull stern (a, b, c, d, e) and the velocity distribution around the stern for Case 1 (f)

In addition, Figure 5f shows the velocity distribution around the stern for Case 1. Similar velocity-distribution plots can be presented for Cases 2, 3, 4, and 5 (not shown). In all cases, the velocity-distribution plots show a decrease in the axial velocity behind the stern, indicating the generation of a wake. The focus of the present study is not on the details of the structure of the turbulent boundary layer (e.g. velocity profiles near the ship's hull) but rather on the gross effect of the fluid flow on the vessel, which is represented by the drag force. The nominal wake fraction representing the wake field is calculated from the mean axial flow velocity behind the ship.

Considering the drag force, Table 4 summarizes the drag coefficient C_D , defined as

$$C_D = \frac{R}{\frac{1}{2}\rho V^2 A} \quad (2)$$

where R is the (calculated) ship's resistance, ρ is the mass density of water, V is the ship's speed, and A is the wetted surface area (WSA). In addition, Table 4 also summarizes the results from the calculations of propeller efficiency for which the wake fractions resulting from the CFD calculations were utilized.

Table 4 Drag coefficient (C_D) and propeller efficiency (η_p)

Case	L_{mb}/L	Stern form	$C_D (\times 10^{-3})$	Increase in C_D (%)	η_p
1	0.11	I	2.70	-	0.656
2	0.34	I	2.71	0.29	0.672
3	0.46	I	2.78	2.69	0.661
4	0.46	II	3.02	8.61	0.612
5	0.46	III	3.14	13.00	0.515

For comparison purposes, the drag coefficient C_D is also calculated according to Holtrop and Mennen (1982) while ignoring the effects of appendages and waves:

$$C_D = C_F(1 + k) + C_A \quad (3)$$

where C_F represents the ITTC-1957 correlation line, $(I+k)$ is a form factor, and C_A is an allowance coefficient. The results are summarized in Table 5.

Table 5 Drag coefficient (C_D) according to Holtrop and Mennen (1982)

Stern form	$C_D (\times 10^{-3})$
V-shaped section	2.23
Normal section	2.27
U-shaped section	3.29

Table 4 shows that an increase in the parallel-middle-body relative length (L_{mb}/L) for ships with the same stern form (Cases 1, 2, and 3) results in an increase in the drag coefficient (0.29–2.69%). For ships with increasingly abrupt stern forms (from a V-like to a U-like form; Cases 3, 4, and 5), the increase in the drag coefficient is much larger (8.61–13.00%). In the latter case, the increase in the drag coefficient is ascribed particularly to the increase in the wake fraction (see Figure 4). Furthermore, the smallest wake fraction results in the most efficient propeller, as expected.

A comparison between Tables 4 and 5 shows that the results for the drag coefficient from CFD lie between those for V-shaped and U-shaped sections calculated from Holtrop and Mennen (1982), as expected. Looking at the values for the drag coefficient calculated from CFD, it can be observed that the stern forms utilized in the CFD simulations are rather U-shaped.

4. CONCLUSION

The relative significance of the parallel-middle-body relative length and stern form in the formation of wake behind single-screw large ships is successfully studied using computational fluid dynamics (CFD). A 10450-DWT tanker is considered as a case study by varying the parallel-middle-body relative length and the ship's stern form. The following conclusions are drawn from the study: (1) An increase in the parallel-middle-body relative length for ships with the same stern form results in an increase in the drag coefficient; (2) A more abrupt stern form (a change from a V-like to a U-like stern form) results in a much larger drag coefficient, ascribed particularly to the larger wake fraction; (3) The stern form affects the nominal wake fraction much more significantly than the parallel-middle-body relative length does; and (4) For a given stern-form section, there is an optimum value for the parallel-middle-body relative length that will result in the smallest wake fraction. CFD can be applied in the early stage of the ship-design process to obtain the optimum stern form and parallel-middle-body relative length.

5. ACKNOWLEDGEMENT

Parts of the present study were presented at the 3rd International Seminar on Ocean and Coastal Engineering, Environmental and Natural Disaster Management (ISOCEEN), 10 December 2015, Surabaya, Indonesia (Suastika & Nugraha, 2017).

6. REFERENCES

- Anderson, J.D., 1995. *Computational Fluid Dynamics: The Basics with Applications*. McGraw-Hill, New York
- Aydin, M., 2013. Development of a Systematic Series of Gulet Hull Forms with Cruiser Stern. *Ocean Engineering*, Volume 58, pp. 180–191

- Banks, J., Phillips, A.B., Turnock, S.R., 2010. Free-surface CFD prediction of components of ship resistance for KCS. *In: The Proceedings of the 13th Numerical Towing Tank Symposium*, 10 October, Duisburg, Germany
- Benedek, Z., Balogh, B., 1968. The Scale Effect on Nominal Wake Fraction of Single-Screw Ships. *Periodica Polytechnica/Mechanical Engineering*, Volume 12(1), pp. 27–37
- Choi, J., Kim, J., Lee, H., Choi, B., Lee, D., 2009. Computational Predictions of Ship-speed Performance. *Journal of Marine Science and Technology*, Volume 14(3), pp. 322–333
- Choi, J.E., Min, K., Kim, J.H., Lee, S.B., Seo, H.W., 2010. Resistance and Propulsion Characteristics of Various Commercial Ships Based on CFD Results. *Ocean Engineering*, Volume 37(7), pp. 549–566
- Dymarski, P., Kraskowski, M., 2010. CFD Optimization of Vortex Generators Forming the Wake Flow of Large Ships. *In: The Proceedings of the 13th Numerical Towing Tank Symposium*, 10 October, Duisburg, Germany
- Dyne, G., 1974. A Study of Scale Effects on Wake, Propeller Cavitation, and Vibratory Pressure at Hull of Two Tanker Models. *In: The SNAME Annual Meeting*, 14–16 November, New York, USA
- Eca, L., Hoekstra, M., 2009. On the Numerical Accuracy of the Prediction of Resistance Coefficients in Ship Stern Flow Calculations. *Journal of Marine Science and Technology*, Volume 14(1), pp. 2–18
- Guldhammer, H., 1962. *Formdata: Some Systematically Varied Ship Forms and their Hydrostatic Data*. Danish Technical Press, Copenhagen
- Hoekstra, M., 1975. Prediction of Full Scale Wake Characteristics Based on Model Wake Survey. *International Shipbuilding Progress*, Volume 22(250), pp. 204–219
- Holden, K.O., Fagerjord, O., Frodstad, R., 1980. Early Design-stage Approach to Reducing Hull Surface Forces Due to Propeller Cavitation. *Transactions SNAME*, Volume 88, pp. 403–442
- Holtrop, J., Mennen, G.G., 1982. An Approximate Power Prediction Method. *International Shipbuilding Progress*, Volume 29(335), pp. 166–171
- Hoyle, J.W., Cheng, B.H., Hays, B., Johnson, B., Nehrling, B., 1986. A Bulbous Bow Design Methodology for High-speed Ships. *Transactions SNAME*, Volume 94, pp. 31–56
- Huang, F., Yang, C., 2016. Hull Form Optimization of a Cargo Ship for Reduced Drag. *Journal of Hydrodynamics*, Volume 28(2), pp. 173–183
- Kostas, K.V., Ginnis, A.I., Politis, C.G., Kaklis, P.D., 2015. Ship-hull Shape Optimazation with a T-Spline Based BEM Isogeometric Solver. *Computer Methods in Applied Mechanics and Engineering*, Volume 284, pp. 611–622
- Larsson, L., Stern, F., Bertram, V., 2003. Benchmarking of Computational Fluid Dynamics for Ship Flows. *Journal of Ship Research*, Volume 47, pp. 63–81
- Melville-Jones, B., 1937. *The Measurement of Profile Drag by the Pitot-Traverse Method*. The Cambridge University Aeronautics Laboratory (R & M No. 1688), Technical Report of the Aeronautical Research Committee for the Year 1935–1936, Volume I
- Menter, F.R., 1994. Two-equation Eddy-viscosity Turbulence Models for Engineering Applications. *AIAA Journal*, Volume 32(8), pp. 1598–1605
- Mitchel, R.R., Webb, M.B., Roetzel, J.N., Lu, F.K., Dutton, J.C., 2008. A Study of the Base Pressure Distribution of a Slender Body of Square Cross Section. *In: The Proceedings of the 46th AIAA Aerospace Sciences Meeting and Exhibition*, 7–10 January, Reno, Nevada, pp. 1–8
- Park, S., Park, S.W., Rhee, S.H., Lee, S.B., Choi, J.-E., Kang, S.H., 2013. Investigation on the Wall Function Implementation for the Prediction of Ship Resistance. *International Journal of Naval Architecture and Ocean Engineering*, Volume 5, pp. 33–46

- Seo, J.H., Seol, D.M., Lee, J.H., Rhee, S.H., 2010. Flexible CFD Meshing Strategy for Prediction of Ship Resistance and Propulsion Performance. *International Journal of Naval Architecture and Ocean Engineering*, Volume 2, pp. 139–145
- Suastika, K., Nugraha, F., 2017. Effects of Parallel-middle-body Relative Length and Stern Form on the Wake Fraction and Ship Resistance. *Applied Mechanics and Materials*, Volume 862, pp. 278–283
- Utama, I.K.A.P., 1999. Investigation of the Viscous Resistance Components of Catamaran Forms. *PhD Thesis*, University of Southampton
- Versteeg, H.K., Malalasekera, W., 2007. *An Introduction to Computational Fluid Dynamics: The Finite Volume Method*. Longman Scientific, Harlow, UK
- Wang, Z.-Z., Xiong, Y., Wang, R., Shen, X.-R., Zhong, C.-H., 2015. Numerical Study on Scale Effect of Nominal Wake of Single Screw Ship. *Ocean Engineering*, Volume 104, pp. 437–451
- Zhao, Y., Zong, Z., Zou, L., 2015. Ship Hull Optimization based on Wave Resistance using Wavelet Method. *Journal of Hydrodynamics*, Volume 27(2), pp. 216–222